Direct and indirect impacts of Saharan dust acting as cloud condensation nuclei on tropical cyclone eyewall development

Henian Zhang,[1,2] Greg M. McFarquhar,[1] William R. Cotton,[3] and Yi Deng[4]

Received 12 January 2008; accepted 12 February 2009; published 20 March 2009.

[1] The mechanisms by which Saharan dust acting as cloud condensation nuclei (CCN) impact tropical cyclone (TC) evolution were examined by conducting numerical simulations of a mature TC with CCN added from lateral boundaries. CCN can affect eyewall development *directly* through release of latent heat when activated and subsequent growth of cloud droplets and *indirectly* through modulating rainband development. Convection in the rainbands was negatively correlated with that in the eyewall in all simulations. The development of rainbands tended to promote latent heat release away from the eyewall, block the surface inflow and enhance cold pools. The maximum impact of rainbands on the eyewall (or vice versa) occurred with a time lag of 3.5 to 5.5 hr. The convection in the eyewall and rainbands did not show a monotonic relationship to input CCN due to the non-linear feedback of heating from a myriad of microphysical processes on storm dynamics. **Citation:** Zhang, H., G. M. McFarquhar, W. R. Cotton, and Y. Deng (2009), Direct and indirect impacts of Saharan dust acting as cloud condensation nuclei on tropical cyclone eyewall development, *Geophys. Res. Lett.*, *36*, L06802, doi:10.1029/2009GL037276.

1. Introduction

[2] During the summer and early fall, North Atlantic tropical cyclones (TCs) are often observed to interact with a hot, dry and dusty air mass originating from the Sahara desert referred to as the Saharan Air Layer (SAL). The SAL can modify the dynamic and thermodynamic environment of TCs, which can either suppress or enhance TC activity [*Dunion and Velden*, 2004; *Karyampudi and Pierce*, 2002]. Dust in the SAL may influence Atlantic TC genesis and development by altering the surface and atmospheric temperature profiles through the absorption and scattering of solar and infrared (IR) radiation [*Karyampudi and Carlson*, 1988; *Lau and Kim*, 2007]. When drawn into TCs, dust may also act as cloud condensation nuclei (CCN), giant CCN (GCCN) and ice nuclei (IN) affecting cloud microphysical processes [*Twohy et al.*, 2009].

[3] *Zhang et al.* [2007] first examined the effect of Saharan dust as nucleating aerosols on TC development using the Regional Atmospheric Modeling System (RAMS), which has a two-moment microphysics scheme with the inclusion of a large cloud droplet mode and explicit CCN activation [*Saleeby and Cotton*, 2004]. Compared to *Rosenfeld et al.* [2007], who turned off the warm rain process to simulate the effect of enhanced CCN, *Zhang et al.* [2007] simulated the actual CCN activation process and found that CCN influenced TC evolution by inducing changes in the cloud droplet number concentration and diameter, and by modifying the eyewall latent heating distribution and thermodynamic structure. The simulated storm intensities were sensitive to the environmental conditions. In this paper, by conducting additional simulations with CCN added at the periphery of a TC, a new physical mechanism is proposed through which large amounts of CCN can influence the eyewall development without directly entering it.

2. Motivation and Numerical Experiments With CCN Added From the Periphery of a TC

[4] In simulations described by *Zhang et al.* [2007], an idealized axisymmetric pre-TC mesoscale vortex was placed in an environment with constant sea surface temperature, zero environmental winds and horizontally uniform temperature and dew point temperature profiles. Three nested domains with horizontal resolutions of 24, 6 and 2 km were used. The numbers of horizontal grid points for Domain 1, Domain 2 and Domain 3 were 80 × 80, 102 × 102 and 152 × 152, respectively. The simulations had varying CCN profiles with CCN maxima of 100 cm^{-3} (Clean), 1000 cm^{-3} and 2000 cm^{-3} between 1 and 5 km, the la yer where dust is typicall y found in the SAL. In this paper, a series of experiments with similar model settings are described where varying amounts of CCN entered a well-developed TC from its lateral boundaries. These simulations resemble the situation where TCs draw dust from a nearby SAL (e.g., Hurricane Felix, 2001) or move into a dust-laden SAL (e.g., Hurricane Bertha, 2008). The output of *Zhang et al.*'s [2007] Clean simulation at 36 hr was used to initialize the new simulations. A well-established eye, eyewall and rainbands were present at that time. CCN were added in Domain 1 and 2, but not in Domain 3 where the storm was located. Five sensitivity experiments, in which CCN with concentrations varying from 250, 500, 1000, 1500 to 2000 cm^{-3} were added to a layer between 1 and 5 km, were conducted and are henceforth denoted B0250, B0500, B1000, B1500 and B2000, where "B" refers to "boundary." To ensure that conclusions reached from this group of simulations were not dependent on the choice of initial condition, four additional groups of simulations were

[1]Department of Atmospheric Sciences, University of Illinois at Urbana-Champaign, Urbana, Illinois, USA.
[2]Now at School of Earth and Atmospheric Sciences, Georgia Institute of Technology, Atlanta, Georgia, USA.
[3]Department of Atmospheric Sciences, Colorado State University, Fort Collins, Colorado, USA.
[4]School of Earth and Atmospheric Sciences, Georgia Institute of Technology, Atlanta, Georgia, USA.

0094-8276/09/2009GL037276$05.00

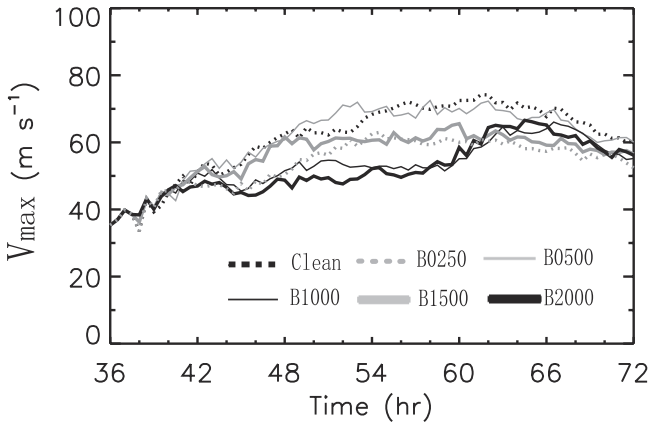

Figure 1. V_{max} for Clean, B0250, B0500, B1000, B1500, and B2000.

conducted with CCN added at 37, 38, 39 and 40 hr to the Domain 1 and 2 of the Clean simulation.

3. Results

[5] Figure 1 shows the evolution of the maximum azimuthally-averaged surface wind speeds (V_{max}) for the six simulations where the time axis starts at 36 hr, the time when CCN were added to Domain 1 and 2. After CCN were introduced, they were gradually transported into the inner domain by winds generated by the vortex itself. The V_{max} started to spread at about 42 hr, six hours after introducing the CCN, and reached a maximum difference of 20 m s^{-1} at 52 hr. The V_{max} from the additional experiments where CCN were introduced at 37, 38, 39 and 40 hr also spread after 6 hours and reached maximum differences of 17, 22, 20, and 17 m s^{-1} at 62, 59, 62 and 60 hr, respectively. Clean was the strongest storm for 52%, 87%, and 53% of the total simulation time for runs with the CCN introduced at 36, 37 and 39 hr, but was neither the strongest nor weakest storm for simulations with the CCN introduced at 38 and 40 hr. Overall, although Clean had a higher V_{max} for 14 out of the 25 simulations which had CCN added from the boundaries, no monotonic relationship between storm intensity and input CCN was found.

[6] As CCN were transported into the vortex, they were activated between cloud base (1 km) and just above the melting level (5 km). The percentage of CCN activated in the model depends upon the vertical velocity, air temperature, CCN median radius and number concentration [*Saleeby and Cotton*, 2004]. Shown in Figure 2, CCN activation was concentrated in two zones: one associated with the eyewall was within approximately 40 km radius from the center, and the other associated with the outward-propagating spiral rainbands was situated outside the 40 km radius. To examine the impact of CCN on different parts of the storm, the inner domain was divided into eyewall and rainbands using the 40 km radius as a threshold, since the wind fields and hydrometeor distribution showed that the majority of the eyewall convection was confined within 40 km radius from the vortex center, except for some ice, snow and aggregates in the convective outflow. Outside the eyewall, CCN number increased dramatically during the first 3 hours and stayed at higher values for larger input CCN (Figure 3a). Two CCN activation episodes associated with the development of rainbands were identified between 42 hr and 57 hr and after 60 hr (Figure 3b). The total activated CCN number in the rainbands monotonically increased with input CCN (Table 1). More cloud droplets with smaller diameters were formed (Figure 3d and Table 1). In contrast to the rainbands, the total CCN number, activated CCN number and associated latent heat release in the eyewall (Figures 3g, 3h, and 3i) did not have the monotonic dependence on input CCN. The total activated CCN number in the eyewall (Table 1) accounted for 30%, 29%, 19%, 13%, 10% and 8% of the total activated CCN number in the rainbands for Clean, B0250, B0500, B1000, B1500, and B2000, respectively. This suggests that a large fraction of CCN input from the boundaries did not reach the eyewall but rather were activated in the rainbands. The mean cloud number concentration (diameter) in the eyewall averaged over the 36 hr did not vary by more than 4% (0.5%) between simulations,

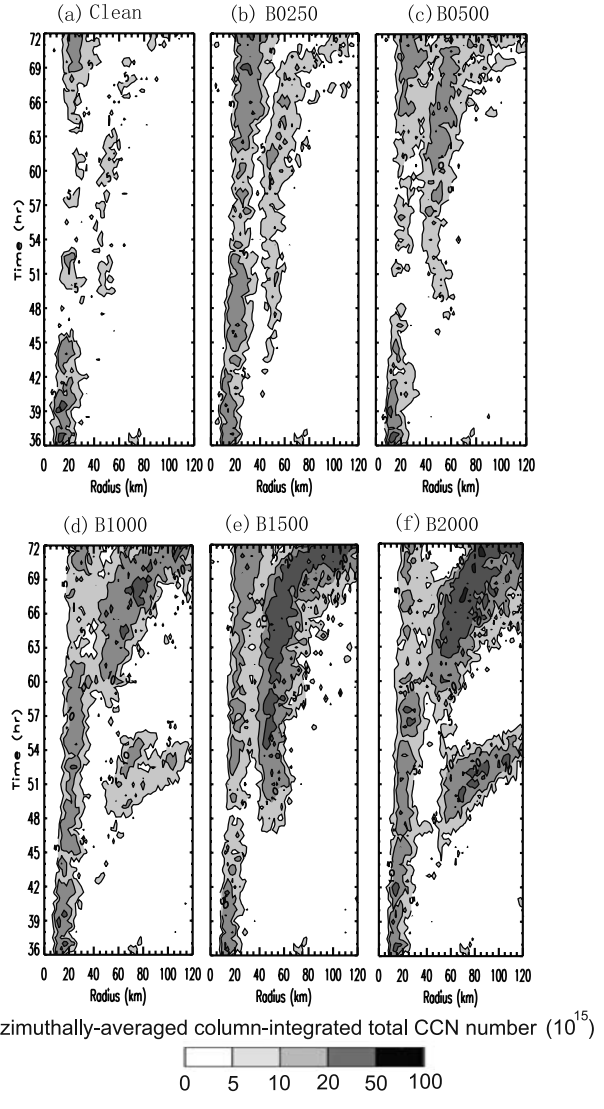

Figure 2. Hovmöller diagrams of azimuthally-averaged column-integrated total activated CCN number for (a) Clean, (b) B0250, (c) B0500, (d) B1000, (e) B1500, and (f) B2000. Contours of 5, 10, 20, 50, and 100 $\times$ 10^{15} are plotted and filled with color from gray to black.

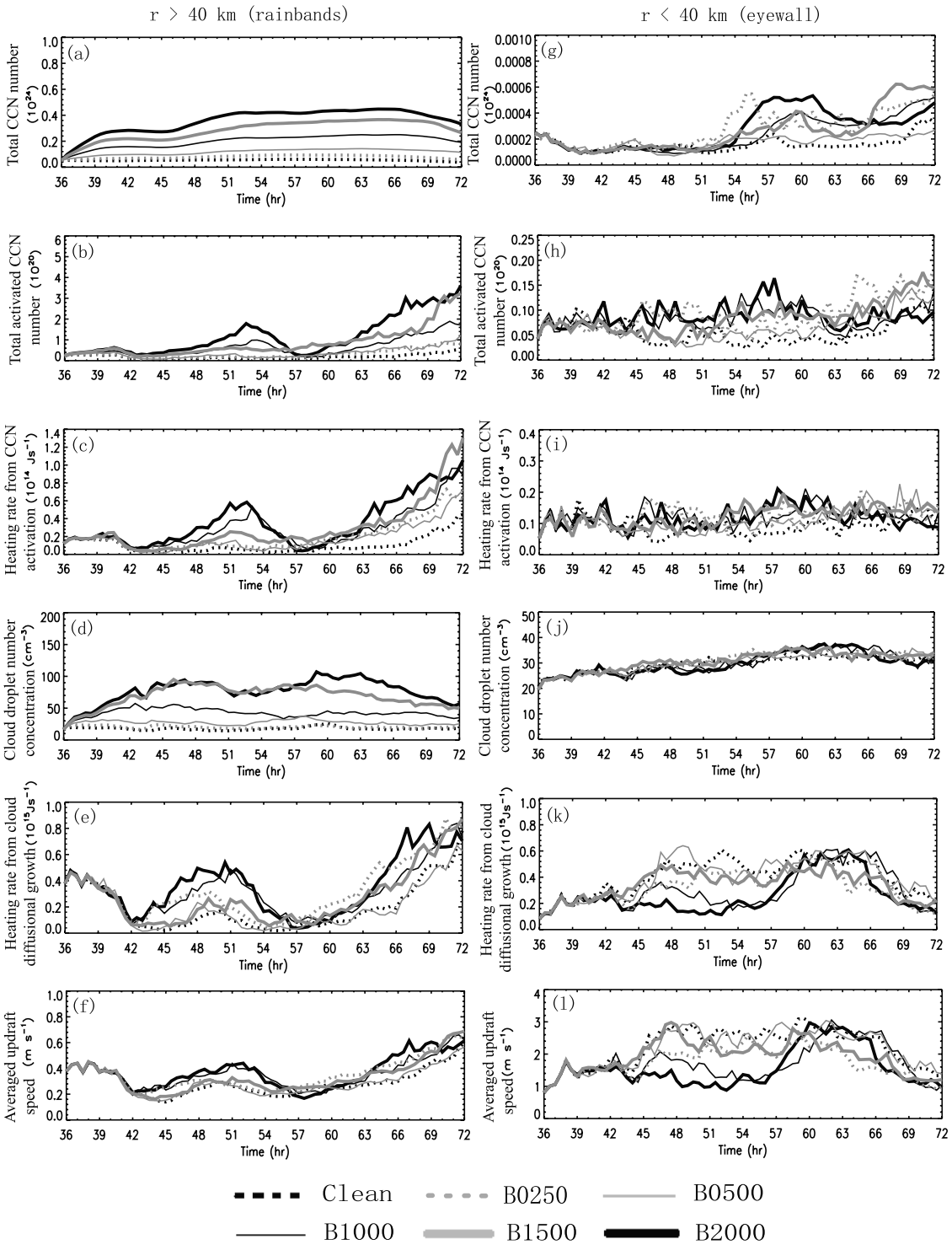

Figure 3. (a) and (g) Temporal evolution of total CCN number, (b) and (h) total activated CCN number, (c) and (i) heating rate from CCN activation, (d) and (j) cloud number concentration, (e) and (k) heating rate from cloud diffusional growth, and (f) and (l) averaged updraft speed for the (left) rainbands and (right) eyewall using the 40 km radius as a threshold.

much smaller than the 331% (26%) variation found in the rainbands (Table 1). The above trends were observed in all the additional simulations with CCN added at various times.

[7] After cloud droplets form through CCN activation, they interact with other hydrometeors through myriads of microphysical processes, which may release latent heat and affect the overall storm development. Of all the latent heating processes examined, including activation of CCN, vapor diffusional growth of hydrometeors, ice nucleation, and freezing of liquid hydrometeors, only the latent heating from CCN activation in the rainbands showed a consistent relationship with the input CCN number. This is not

Table 1. Statistics of Selected Variables for the Eyewall and Rainbands

Variables	Clean	B0250	B0500	B1000	B1500	B2000
			Total Activated CCN Number, 10^{20}			
Eyewall	4.09	6.72	4.84	6.09	6.19	6.44
Rainbands	13.79	22.8	25.6	46.98	61.74	84.67
			Latent Heat Released by CCN Activation, 10^{18} J			
Total	2.6	4.2	3.71	5.23	5.38	6.18
Eyewall	1.25	1.6	1.43	1.56	1.63	1.56
Rainbands	1.35	2.6	2.29	3.68	3.75	4.62
			Cloud Number Concentration, cm^{-3}			
Eyewall	29.6	30.5	30	30	30.7	29.8
Rainbands	17.8	20.3	27.3	42.5	68.8	76.8
			Cloud Mean Diameter, μm			
Eyewall	38.9	38.6	38.8	38.7	38.7	38.7
Rainbands	35.1	34.4	32.3	31.5	27.8	29
			Latent Heat Released by Cloud Diffusional Growth, 10^{19} J			
Total	7.85	8.42	7.84	8.17	8.03	8.12
Eyewall	5.28	4.22	5.28	3.96	4.49	3.43
Rainbands	2.57	4.21	2.56	4.22	3.54	4.68
			Correlation Coefficient Of Latent Heat Released by Cloud Diffusional Growth Between Eyewall Rainbands			
zero time lag	−0.63	−0.53	−0.47	−0.21	−0.58	−0.29
Maximum (corresponding time lag - rainband led eyewall)	−0.81 (4.5 hr)	−0.79 (5.5 hr)	−0.84 (5 hr)	−0.78 (5 hr)	−0.88 (4.5 hr)	−0.68 (4 hr)
			Correlation Coefficient of Averaged Updrafts Between Eyewall and Rainbands			
Zero time lag	−0.61	−0.63	−0.49	−0.24	−0.63	−0.28
Maximum (corresponding time lag - rainband led eyewall)	−0.84 (3.5 hr)	−0.83 (5 hr)	−0.86 (4 hr)	−0.74 (4.5 hr)	−0.88 (3.5 hr)	−0.64 (3.5 hr)
			Total Precipitation, 10^{10} m^3			
Total	1.00	1.08	1.03	1.07	1.06	1.07
Eyewall	0.77	0.67	0.64	0.67	0.71	0.59
Rainbands	0.23	0.41	0.39	0.4	0.35	0.48

surprising since the other microphysical processes are not simple functions of CCN. For example, the diffusional growth of cloud droplets, which contributes over 70% to the total latent heat, would increase with increasing cloud droplet number concentration and diameter if other environmental parameters are constants [*Walko et al.*, 1995]. Since adding CCN leads to an increase in cloud number concentration but a decrease in cloud droplet diameter, the ultimate latent heat from cloud diffusional growth was not simply related to the initial CCN. Further, environmental parameters such as temperature and water vapor mixing ratio were ever-changing as a result of variations in the microphysical and thermodynamical processes. Thus, neither in the rainbands nor in the eyewall did heating induced by cloud diffusional growth show a clear relationship with CCN (Figures 3e and 3k and Table 1).

[8] As the major latent heating term, the heating rate from cloud diffusional growth in the rainbands (Figure 3e) and eyewall (Figure 3k) was highly correlated with the averaged updrafts in those regions (Figures 3f and 3l) with correlation coefficients greater than 0.85 significant at the 95% level. The correlation coefficients between the latent heat released by cloud diffusional growth (as well as averaged updrafts) in the eyewall and that in the rainbands were negative for all six simulations (Table 1). The absolute values of the time-lag correlation coefficients monotonically increased with increasing time lag that rainbands led the eyewall and reached maxima when the time lag was 3.5 to 5.5 hrs (Table 1). The negative correlation and monotonic increase with increasing time lag before reaching maxima were found in all additional groups of simulations with CCN added at 37, 38, 39, and 40 hr, with the maximum correlation occurring at a time lag between 3.5 and 5.5 hr. This negative correlation and time lag indicates that if convection in the rainbands increases, then convection in the eyewall likely decreases (and vice versa), with the rainband convection having its maximum impact on the eyewall convection (and vice versa) after about 3.5 to 5.5 hr.

[9] The formation mechanism of the spiral rainbands has been proposed to be associated with the vortex Rossby waves breaking and merging processes [e.g., *Guinn and Schubert*, 1993; *Wang*, 2002]. Spiral rainbands have been hypothesized to strengthen the eyewall by transferring cyclonic potential vorticity (PV) into it under certain circumstances [*May and Holland*, 1999] or to weaken it by promoting convection outside the eyewall and introducing

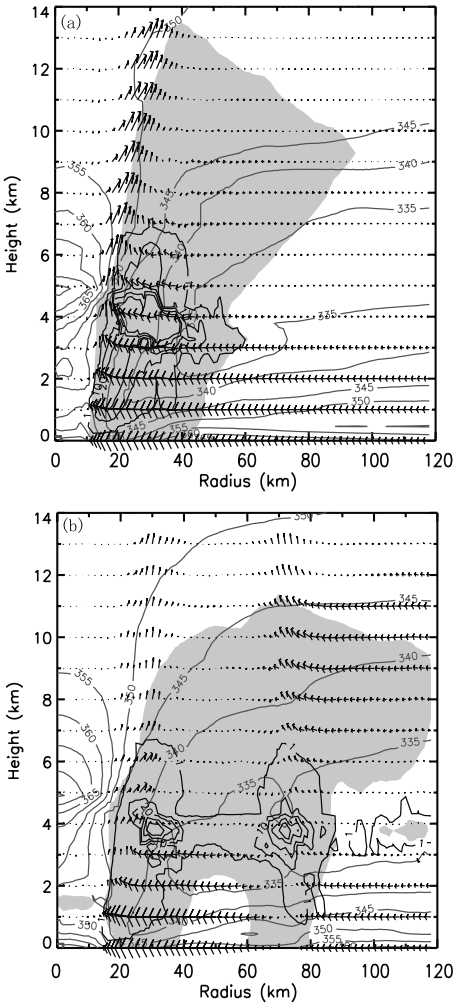

Figure 4. Azimuthally-averaged wind field (vector), θ_e (contoured with an interval of 5 K and colored in dark gray), mixing ratio of the total condensate (with contour of 0.5 g kg^{-1} filled with color gray), and latent heating from cloud diffusional growth (with contours of 1, 10, 20, 40, and 60 K hr^{-1} in color black) for B2000 at (a) 60 hr and (b) 70 hr.

air with low equivalent potential temperature (θ_e) to the boundary layer inflow [*Barnes et al.*, 1983; *Powell*, 1990]. In our simulations, the development of the rainbands tends to support convection and diffusional growth of cloud droplets outside of the eyewall, enhance cold pools by producing downdrafts and evaporative cooling of rain, and block the surface radial inflow transporting high θ_e air into the eyewall. Thus, the overall impact of rainbands on the eyewall is similar to that of secondary eyewalls on the primary eyewall [*Willoughby et al.*, 1982]. This mechanism is illustrated in Figure 4, using B2000 as an example. At 60 hr, when rainbands were not intense, surface inflow with high θ_e air directly reached the eyewall, and strong updrafts and intense latent heating from cloud diffusional growth were found in the eyewall. At 70 hr, intense rainbands were located between 60 and 80 km in the radial direction. The radial inflow with high θ_e air went into the rainbands first and promoted convection and cloud formation there. The air near the surface underneath the rainbands had lower θ_e compared to the environment, which led to the formation of a cold pool outside the eyewall. This is consistent with previous observations by *Barnes et al.* [1983] and *Powell* [1990].

[10] The negative correlation of the diffusional growth of cloud droplets (and mean updraft intensity) between the eyewall and rainbands in our simulations suggests that overall, the rainbands hinder eyewall development. Further, the maximum impact of rainbands on the eyewall (and vice versa) has a time delay of 3.5 to 5.5 hr. However, even though there is a negative correlation between the convective intensity in the rainbands and eyewall and a positive relation between the CCN activated in the rainbands and the input CCN, neither eyewall nor rainband intensities were monotonically related to the input CCN. This results from the lack of a clear relationship between cloud diffusional growth and other microphysical processes with input CCN and the nonlinear feedback of heating from these processes on the storm dynamics.

4. Conclusion and Discussion

[11] Idealized simulations introducing CCN into the initial environment of a pre-TC vortex and into a mature TC from its lateral boundaries have been discussed by *Zhang et al.* [2007] and here to examine the potential impact of Saharan dust acting as CCN on TC evolution. By adding CCN within the initial environment, CCN *directly* affect the early eyewall evolution by varying distributions of latent heat, and hence trigger variations in dynamic and thermodynamic processes that ultimately modify eyewall intensity. When CCN were added from the boundaries, higher input CCN concentration led to more activated CCN, and more cloud droplets with smaller diameters, but only in the rainbands. The amount of CCN that reached the eyewall was not monotonically related to the input CCN. The total heat released by cloud diffusional growth, the major latent heating term, in both the eyewall and rainbands did not show any monotonic relation with the input CCN concentration. Similarly, the storm intensity (measured by the V_{max} and averaged updrafts in the eyewall) and the rainband intensity (measured by the averaged updrafts) did not show a monotonic relationship with input CCN. In all simulations, a negative correlation of convective intensity in the eyewall with that in the rainbands was found, and the absolute values of the correlation coefficients reached maxima when the rainbands led the eyewall by 3.5 to 5.5 hr. Intense convection in developing rainbands can adversely affect eyewall intensification by causing latent heat to be less concentrated from the eyewall, enhancing cold pools and blocking the surface radial inflow. Thus, the CCN *indirectly* affected the eyewall by modulating rainband development, but in a way that did not systematically depend on input CCN. Except for CCN activation, all the examined microphysical processes that contribute to latent heating did not show a simple relationship with input CCN. The impact of nucleating aerosols on TC intensity is complicated owing to the nonlinear interaction between aerosol, hydrometeors and the environment through a myriad of microphysical processes and complex feedback of heating from these processes on the storm dynamics. Moreover, impact of dust acting as nucleating aerosols on

TC development could be subjected to dry air in the SAL and strong wind shear. In addition, dust acting as IN can also directly/indirectly affect the TC eyewall development in a similar manner, which needs to be examined in the future. The relative importance of environmental CCN and IN needs to be evaluated with regard to all environmental factors that can affect TC development.

[12] **Acknowledgments.** This work was sponsored by the NASA Earth System Science (ESS) Fellowship, grant NNG04GQ99H, and by the Tropical Cloud Systems and Processes (TCSP) mission, grant NNG05GR61G. The authors would like to thank R. M. Rauber, B. F. Jewett, M. S. Gilmore, and J. A. Curry for their help and support.

References

Barnes, G., E. Zipser, D. Jorgensen, and F. Marks (1983), Mesoscale and convective structure of a hurricane rainband, *J. Atmos. Sci.*, *40*, 2125–2137.

Dunion, J. P., and C. S. Velden (2004), The impact of the Saharan air layer on Atlantic tropical cyclone activity, *Bull. Am. Meteorol. Soc.*, *85*, 353–365.

Guinn, T. A., and W. H. Schubert (1993), Hurricane spiral bands, *J. Atmos. Sci.*, *50*, 3380–3403.

Karyampudi, V. M., and T. N. Carlson (1988), Analysis and numerical simulations of the Saharan air layer and its effect on easterly wave disturbances, *J. Atmos. Sci.*, *45*, 3102–3136.

Karyampudi, V. M., and H. F. Pierce (2002), Synoptic-scale influence of the Saharan air layer on tropical cyclogenesis over the eastern Atlantic, *Mon. Weather Rev.*, *130*, 3100–3128.

Lau, K. M., and J. M. Kim (2007), How nature foiled the 2006 hurricane forecasts, *Eos Trans. AGU*, *88*, 105–107.

May, P. T., and G. J. Holland (1999), The role of potential vorticity generation in tropical cyclone rainbands, *J. Atmos. Sci.*, *56*, 1224–1228.

Powell, M. D. (1990), Boundary layer structure and dynamics in outer hurricane rainbands. Part I: Mesoscale rainfall and kinematic structure, *Mon. Weather Rev.*, *118*, 891–917.

Rosenfeld, D., A. Khain, B. Lynn, and W. L. Woodley (2007), Simulation of hurricane response to suppression of warm rain by sub-micron aerosols, *Atmos. Chem. Phys. Discuss.*, *7*, 5647–5674.

Saleeby, S. M., and W. R. Cotton (2004), Large-droplet mode and prognostic number concentration of cloud droplets in the Colorado State University Regional Atmospheric Modeling System (RAMS). Part I: Module descriptions and supercell test simulations, *J. Appl. Meteorol.*, *43*, 182–195.

Twohy, C. H., et al. (2009), Saharan dust particles nucleate droplets in eastern Atlantic clouds, *Geophys. Res. Lett.*, *36*, L01807, doi:10.1029/2008GL035846.

Walko, R. L., W. R. Cotton, M. P. Meyers, and J. Y. Harrington (1995), New RAMS cloud microphysics parameterization. Part I: The single-moment scheme, *Atmos. Res.*, *38*, 29–62.

Wang, Y. (2002), Vortex Rossby Waves in a numerically simulated tropical cyclone. Part I: Overall structure, potential vorticity, and kinetic energy budgets, *J. Atmos. Sci.*, *59*, 1213–1238.

Willoughby, H. E., J. A. Clos, and M. G. Shoreibah (1982), Concentric eye walls, secondary wind maxima, and the evolution of the hurrican vortex, *J. Atmos. Sci.*, *39*, 395–411.

Zhang, H., G. M. McFarquhar, S. M. Saleeby, and W. R. Cotton (2007), Impacts of Saharan dust as CCN on the evolution of an idealized tropical cyclone, *Geophys. Res. Lett.*, *34*, L14812, doi:10.1029/2007GL029876.

W. R. Cotton, Department of Atmospheric Sciences, Colorado State University, Fort Collins, CO 80523-1371, USA.

Y. Deng and H. Zhang, School of Earth and Atmospheric Sciences, Georgia Institute of Technology, Atlanta, GA 30305, USA. (henian.zhang@eas.gatech.edu)

G. M. McFarquhar, Department of Atmospheric Sciences, University of Illinois at Urbana-Champaign, Urbana, IL 61801-3070, USA.